181-190.
Lau, C., and Richards, F. M. (1976), submitted for publication.
Laemmli, U. K. (1970), *Nature (London) 227,* 680-685.
Lehninger, A. (1972), Biochemistry, New York, N.Y., Worths Publisher Inc., p 31.
Luria, S. E. (1964), *Ann. Inst. Pasteur, Paris 107,* 63-73.
Means, G. E., and Feeney, R. G. (1968), *Biochemistry 7,* 2192-2194.
Nomura, M. (1963), *Cold Spring Harbor Symp. Quant. Biol. 28,* 315-324.
Ohsumi, Y., and Imahori, K. (1974), *Proc. Natl. Acad. Sci. U.S.A. 71,* 4062-4066.
Olsnes, S., and Pehl, A. (1973), *Eur. J. Biochem. 35,* 179-185.
Olsnes, S., Refsnes, K., and Phil, A. (1974), *Nature (London) 249,* 627-631.
Peacock, A. C., and Dingman, C. W. (1968), *Biochemistry 7,* 668-674.
Sabet, S. F., and Schnaitman, C. A. (1972), *J. Biol. Chem. 248,* 1797-1806.
Samson, A. C. R., Senior, B. W., and Holland, I. B. (1972), *J. Supramol. Struct. 2,* 135-144.
Saxe, L. (1975), *Biochemistry 14,* 2058-2063.
Spero, L., Metzger, J. F., Warren, J. R., Gryzin, B. Y. (1975), *J. Biol. Chem. 250,* 5026-5032.
Weber, K., and Osborn, M. (1969), *J. Biol. Chem. 244,* 4406-4412.
Webster, R. E., Engelhardt, D. L., Konigsberg, W., and Zinder, N. D. (1967), *J. Mol. Biol. 29,* 27-43.
Weiner, A. M., Platt, T., and Weber, K. (1972), *J. Biol. Chem. 247,* 3243-3251.

Assignment of a Ligand in Stellacyanin by a Pulsed Electron Paramagnetic Resonance Method†

W. B. Mims* and J. Peisach‡

ABSTRACT: The electron spin echo decay envelope for the blue copper protein, stellacyanin, and for a number of other Cu(II) complexes has been studied. Particular attention was given to the form of the "nuclear modulation" patterns, which show the effects of coupling between the electron spin and the neighboring nuclei. The envelopes for the hydrated cupric complex and for copper(II) glycylglycine were essentially the same and indicative of the coupling to protons. The peptide complex contains nitrogen nuclei coupled directly to Cu(II), but the coupling constant is so large for these nuclei that a modulation pattern ascribable to ^{14}N is not seen. For copper(II) bovine serum albumin, on the other hand, a contribution due to the coupling of the remote nitrogen belonging to a histidyl imidazole ligand was observed. The modulation pattern for this complex and for stellacyanin closely resembled one another, strongly suggesting that an imidazole is ligated to the copper in this blue protein.

Two types of mononuclear copper sites have been identified in copper proteins. Of these, the widest attention has been given to the dark blue, type I site, as is found in azurin (Suzuki and Iwasaki, 1962; Sutherland and Wilkinson, 1963; Gould and Mason, 1967; Brill et al., 1968), stellacyanin (Omura, 1961; Peisach et al., 1967), plastocyanin (Katoh et al., 1962; Blumberg and Peisach, 1966), umecyanin (Stigbrand et al., 1971), and a variety of copper-containing oxidases (Malmström and Vänngård, 1960; Blumberg et al., 1963, 1964, Poillon and Dawson, 1963; Nakamura and Ogura, 1966; Malkin et al., 1968a,b; Malmström et al., 1968; Nakamura et al., 1968; Andréasson and Vänngård, 1970). This is in part because of the unusual optical and magnetic properties associated with them. They are generally characterized by an extraordinarily intense optical absorption near 600 nm and a small value of the magnetic hyperfine coupling constant $A_\parallel$. Simple copper peptide complexes and copper in type II sites are, on the other hand, characterized by values of $A_\parallel$ several times larger and also are less intensely colored (Malkin and Malmström, 1970).

A comparison of the EPR[1] data for copper proteins and model compounds suggests that the metal ligands for type II sites in copper-containing oxidases are oxygen and/or nitrogen, sulfur being ruled out (Peisach and Blumberg, 1975). EPR studies on type I sites have not, however, provided any definite information regarding ligands and most of the evidence has been obtained by chemical means. One such study performed with parsley plastocyanin, a blue copper protein containing a single cysteinyl residue, strongly implicates cysteinyl sulfur as a ligand (Finazzi-Agró et al., 1970). Removal of the copper activates the cysteinyl sulfur for binding to *p*-mercuribenzoate. While in this mercurial-bound form, the protein cannot be reconstituted to the holoprotein with copper. Removal of the

† From Bell Laboratories, Murray Hill, New Jersey 07974 (W.B.M.), and the Departments of Pharmacology and Molecular Biology, Albert Einstein College of Medicine, Yeshiva University, Bronx, New York 10461 (J.P.). *Received April 7, 1976.* The portion of this investigation carried out at the Albert Einstein College of Medicine was supported in part by United States Public Health Service Research Grant HL-13399 from the Heart and Lung Institute. This is Communication No. 350 from the Joan and Lester Avnet Institute of Molecular Biology.

‡ Recipient of Public Health Service Research Career Development Award 2-K3-GM31,156 from the National Institute of General Medical Sciences.

[1] Abbreviations used are: EPR, electron paramagnetic resonance; ENDOR, external nuclear double resonance; Cu(II)(imid)$_4$, copper tetraimidazole; Cu(II)(guan)$_4$, copper tetraguanidine.

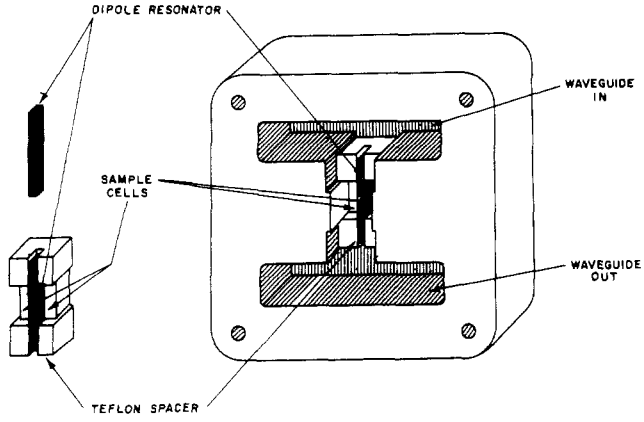

FIGURE 1: Sketch of the microwave cavity used in the experiments. The resonant element consists of a brass strip $\simeq \frac{1}{2}$ wavelength long. The strip is 10.2-mm long and the central slot in which it is located is 12.7-mm long. The cavity is mounted at the end of two X band waveguides tapered down along the narrow dimension to a cross section of 22.9 × 5.1 mm. The ends of the resonator couple to the microwave electric field in the tapered waveguide sections. The sample is placed in the well situated at the center of the resonator where the microwave magnetic field is maximum. The complete unit is mounted horizontally with the Zeeman field in the plane of the paper.

mercurial permits reconstitution. Some physical evidence indicating that sulfur is a ligand was obtained by McMillin and co-workers (1974) who substituted Co(II) for Cu(II) in stellacyanin, thus shifting the strong 600-nm optical absorption to 355 nm. This transition is known to be associated with $RS^- \rightarrow Co(II)$ charge transfer. The authors argued that the major visible absorption at 604 nm in the copper-containing protein should be ascribed to the corresponding $RS^- \rightarrow Cu(II)$ charge transfer transition.

Although these studies point to the conclusion that one ligand in the type I copper sites is sulfur, the nature of the other ligands has not been determined. A limited amount of information, however, has been obtained by ENDOR measurements. Rist et al. (1970) reported on radio frequency absorption in stellacyanin at $\simeq$17 MHz that they attributed to nitrogen ligands of the copper. But they were unable from their results to ascertain what nitrogen-containing group was involved.

In the present communication, we describe measurements of the electron spin echo envelope for stellacyanin and for a number of other copper compounds. The results demonstrate that an imidazole, presumably from an histidine residue, is bound to the copper of stellacyanin.

Materials and Methods

Copper-containing model compounds were prepared either from cupric acetate (Mallinckrodt), cupric chloride (Mallinckrodt), or cupric perchlorate (Alfa Inorganic). The aquo-Cu(II) complex was prepared by dissolving the perchlorate in water (20 mM), adjusting the pH to 1.0 with perchloric acid, and diluting with an equal volume of glycerol.

Copper glycylglycine was prepared from copper acetate (18 mM) to which glycylglycine (Sigma) was added (final concentration, 20 mM) and the pH was adjusted to 8.5 with NaOH. An equal volume of glycerol was added.

Copper hexaglycine (Sigma) was prepared by adding a stochiometric equivalent of the peptide to a 20 mM solution of cupric acetate and raising the pH to 6.0 with NaOH before diluting with an equal volume of glycerol. Other samples of the complex were prepared at pH 7.0 and 9.5.

Copper–albumin complex was prepared by adding cupric acetate (final concentration 1.8 mM) to a 2.0 mM solution of bovine serum albumin (Calbiochem) in 50 mM phosphate buffer, pH 7.4.

Copper tetraimidazole ($Cu(II)(imid)_4$) and copper tetraguanidine ($Cu(II)(guan)_4$) complexes were in each case prepared by adding a 40-fold molar excess of the ligand (Eastman Organic) together with an equal volume of glycerin to 20 mM cupric acetate and adjusting the pH to 8.0.

Stellacyanin was prepared using a modification of the method of Reinhammar (1970). *Rhus vernicifera* acetone powder (175 g), prepared by Saito and Co., Ltd., Tokyo, was homogenized in small batches with 3.5 l. of 0.01 M potassium phosphate buffer, pH 6.0, in a Waring blender run at medium speed for 2-min intervals at 4 °C. The homogenate was stirred overnight and was filtered on a Buchner funnel using Whatman No. 3 filter paper. The filtrate was centrifuged at 15 000*g* for 20 min and was refiltered using Whatman No. 1 paper. The second filtration was required to remove trace particles that tended to clog chromatographic columns used in the procedure.

The clear, green filtrate was applied to a 7.5 × 26 Whatman CM 52 cation exchange resin equilibrated with the same phosphate buffer. Both the conductivity and pH were used to ascertain buffer equilibration with the resin. During the loading of the column, a dark blue band concentrated at the top and yellow material that was not absorbed passed through in the holdup volume. The column was then washed with 4 l. of 0.01 M potassium phosphate buffer, pH 6.0 until the absorption at 250 nm (1-cm light path) was less than 0.005. The buffer concentration was next raised to 0.05 M, and laccase, which appeared as a dark blue solution absorbing in the visible at 613 nm, began to elute after roughly 750 ml. Approximately 1850 ml of buffer was required to remove the laccase completely from the column as judged from the 250-nm absorption. Buffer concentration was then raised to 0.1 M and the stellacyanin that absorbed at 604 nm began to elute after the addition of 1100 ml of buffer. Approximately 2200 ml of buffer was required for the complete elution of this fraction.

The $A_{604/280}$ spectral ratio for stellacyanin obtained by this procedure was measured with a Cary Model 14R spectrophotometer and found to be 0.161, in good agreement with previously published values (Peisach et al., 1967). Using a standard, *p*-phenylenediamine assay (Peisach and Levine, 1965), the oxidase activity of stellacyanin was determined to be one five-thousandths that of a laccase sample giving the same optical absorption at 613 nm.

The protein was concentrated and dialyzed against 0.01 M potassium phosphate buffer, pH 7.0, under pressure using Amicon UM2 filters. The solution used in the experiments was 3.4 mM as judged from the extinction at 604 nm (Peisach et al., 1967).

Electron-spin-echo measurements were performed at X band ($\simeq$9 GHz) and at a temperature of 4.2 K. The apparatus was a modification of one described by Mims (1974). The cavity is of a novel design and is shown schematically in Figure 1. The resonating element consists of a strip of brass approximately one-half wavelength long, coupled at each end to the microwave electric field in sections of X band waveguide tapered along the narrow dimension. The sample is located in a well cut in the Teflon spacer and occupies a region in which the microwave magnetic field is at a maximum. The cavity-filling factor for this arrangement is exceptionally high and helps to offset the loss in signal intensity that results from working with a glassy sample whose EPR spectrum is spread out over a range of Zeeman fields.

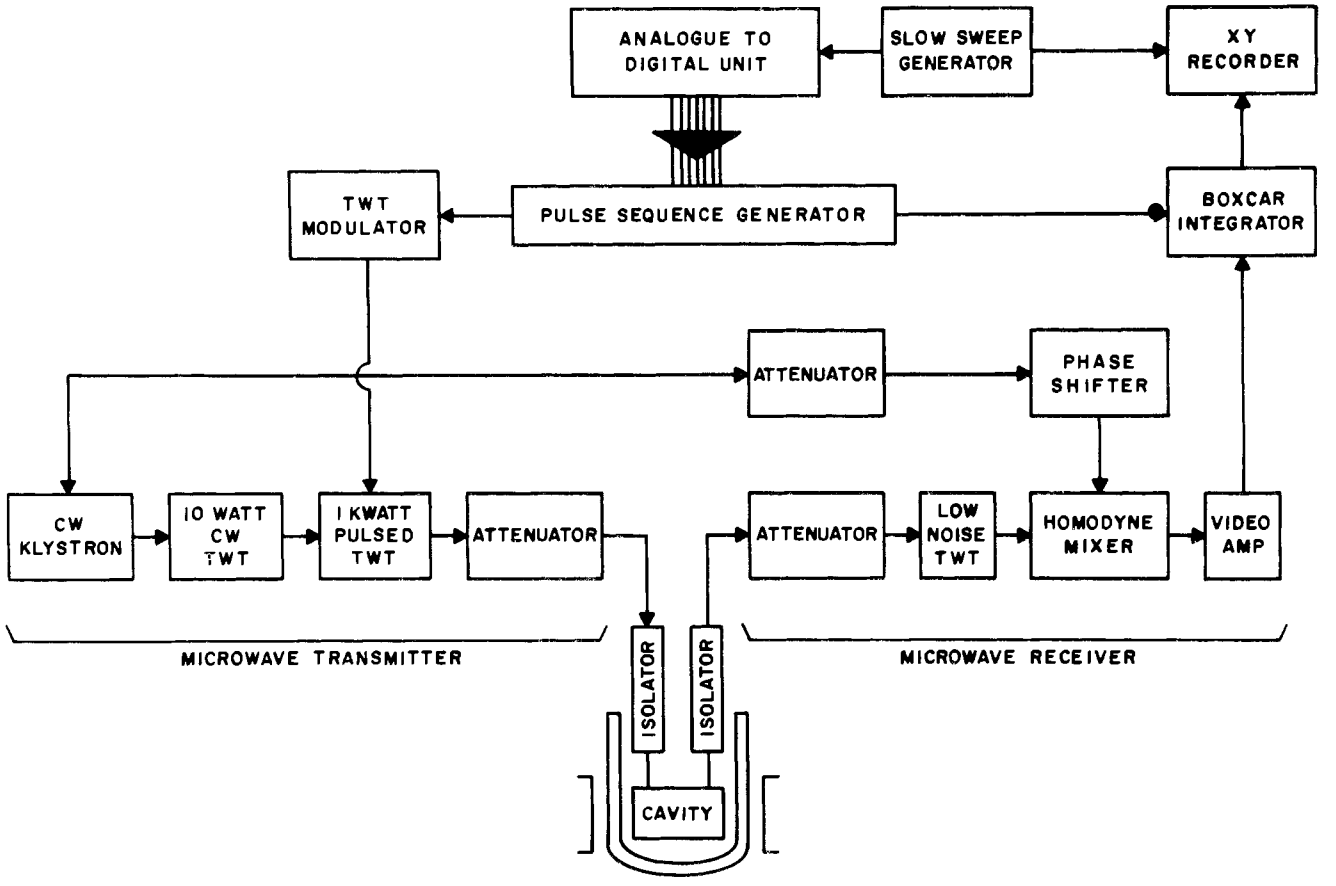

FIGURE 2: Block schematic of the electron spin-echo apparatus. For the cavity see Figure 1. A digital voltmeter with BCD output was used as the analogue to digital unit. This unit was used to program two BNC Model 7030 digital delay generators that formed the principal element in the pulse sequence generator.

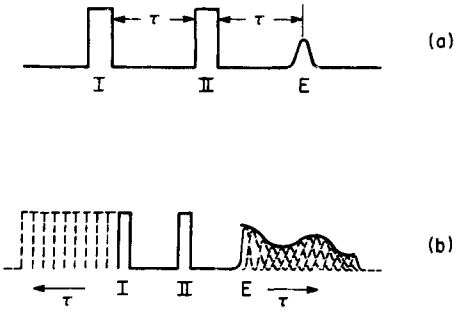

FIGURE 3: (a) Two pulse electron spin-echo sequence consisting of microwave pulses (I and II), and spin echo signal (E). The time, τ, is the period between applied pulses and between the second applied pulse and the spin echo. In the experiments described here the microwave pulses were each 20 ns. long and the power level 0.1–1.0 kW. (b) Superposition of a number of electron spin-echo signals illustrating meaning of the envelope modulation function, As τ is increased the amplitude of the echo signal varies, giving rise to the modulation patterns shown in Figures 4–9. For a more complete description see Mims, 1972c.

The block schematic of the spin-echo spectrometer is shown in Figure 2. The microwave transmitter consists of a Litton L5022 1 kW pulsed traveling wavetube (TWT), modulated by a unit whose active element consists of a Tung-Sol 8455 secondary emission tube. A Watkins Johnson WJ491-35 microwave TWT amplifier constitutes the first stage of the receiver system. This is followed by a homodyne detection mixer and a wide-band (150 MHz) Keithley 107 pulse amplifier. Echo signals are collected and averaged by means of a "boxcar circuit". The timing pulses for the spin-echo sequence (Figure 3a, see below) and for the boxcar gate were provided by a pulse generator and by two BNC Model 7030 programmable digital delay units ("pulse sequence generator"). One unit was used to generate the interval τ between pulses I and II and the other unit to generate the equivalent interval τ between pulse II and the boxcar trigger. The two units were programmed from the BCD output of a digital voltmeter (Newport Laboratories Model 2000 A/S, shown in Figure 2 as "analogue to digital unit") that was driven by a linear ramp waveform ("slow sweep generator"). The same linear ramp provided the X axis drive for the X-Y recorder (Hewlett Packard Model 7004B) with which Figures 4–10 were obtained.

Discussion

The envelope of electron spin echos is the function obtained by plotting the amplitude of the spin-echo signal against the time between the echo-generating microwave pulses (Figure 3a). In this function it is often possible to observe a periodic "modulation" that can be shown to arise from superhyperfine structure (shfs) in the resonance line (Figure 3b) (Rowan et al., 1965; Zhidomirov and Salikov, 1968; Yudanov et al., 1968; Grischkowsky and Hartmann, 1970; Liao and Hartmann, 1972; Newman and Rowan, 1972; Mims, 1972a, 1972b; Narayana et al., 1975; Kevan et al., 1975). The echo envelope is therefore capable of yielding information of the same kind as that which is obtained in ENDOR experiments, although the factors which determine the relative amplitudes of the superhyperfine (shf) frequencies are somewhat different from those which determine the line intensities in an ENDOR spectrum.

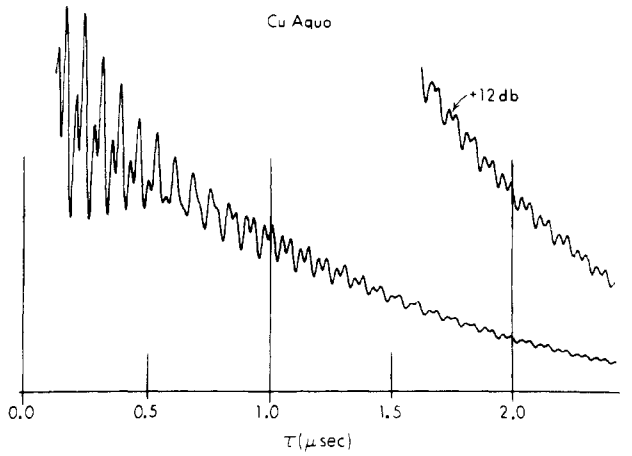

FIGURE 4: Envelope modulation function for Cu(II)–aquo complex illustrating effect due to coupling between Cu(II) and surrounding protons. Curves were obtained at 4.2 K and at a frequency of 9.014 GHz. The spin-echo recurrence rate was ≃180 Hz. Recordings were obtained by slowly increasing τ from ≃0.14 to ≃2.4 μs in a total time ≃300 s.

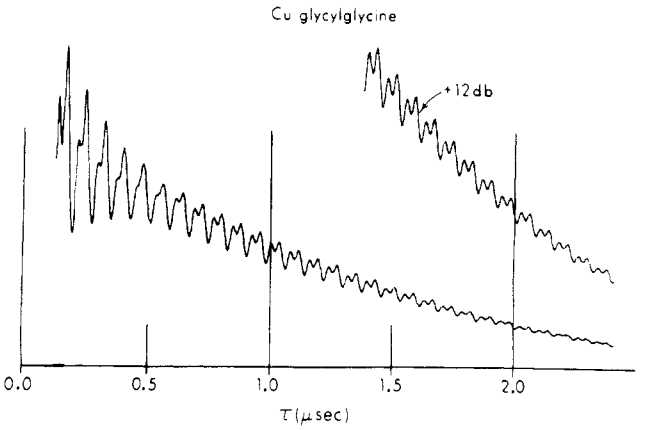

FIGURE 5: Envelope modulation function for Cu(II)–glycylglycine. Conditions were similar to those in Figure 4. The effect of proton coupling is almost the same as in Figure 4. Coupling between Cu(II) and the directly coordinating ^{14}N nucleus yields no visible effect in this experiment. This is because the term A I·S dominates other terms in that portion of the spin Hamiltonian that describes the interactions of the ^{14}N nucleus.

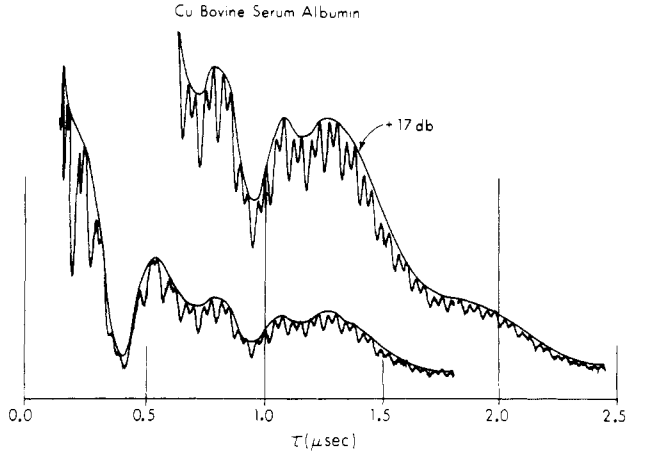

FIGURE 6: Envelope modulation function for the complex formed between Cu(II) and bovine serum albumin measured at the $g_\perp$ end of the EPR spectrum. Conditions were similar to those in Figure 4. The low-frequency period shown by the line joining the proton peaks is due to coupling with the ^{14}N nucleus belonging to the N-1 nitrogen in the imidazole ligand (^{14}N nuclei immediately adjacent to the Cu(II) ion do not contribute to the envelope in this type of experiment. (See Figure 5.))

The modulation effect arises as a result of interference between allowed and semiallowed EPR transitions that are coherently excited by the microwave pulses. The theory of the effect is given in detail in the above references (see in particular Rowan et al., 1965; Mims, 1972a). For the present purpose one of its more important predictions concerns the relationship between the nuclear terms in the spin Hamiltonian, the electron–nuclear coupling term, and the depth of the modulation pattern. When there is a wide disparity between the nuclear Zeeman and nuclear quadrupole terms, and the electron–nuclear coupling term S·A·I, the modulation pattern will either be shallow or fail to show up at all. (See Mims, 1972a, section VI.) Under these conditions there is a clear distinction between allowed and forbidden transitions, thus eliminating the possibility of interference effects. This property has proved to be especially useful in the present study, since, as we show later, it has enabled us to discriminate between strongly coupled nitrogen nuclei directly coordinated with the copper and other more weakly coupled nitrogen nuclei occurring in the ligands.

The measurement itself is straightforward enough but the analysis of the envelope function in terms of a frequency spectrum presents serious difficulties. This is largely because one cannot record the initial portion of the envelope corresponding to the time taken by the experimental equipment to recover from the second microwave pulse (Figure 3a) (Blumberg et al., 1973). Fortunately, in the present set of experiments we have been able to dispense with this problem altogether by making direct comparisons between the recorded envelope functions for stellacyanin and a number of other copper complexes.

Figure 4 shows the electron spin echo envelope for the Cu(II)–aquo complex as recorded at a magnetic field setting in the vicinity of $g_\parallel$ (Walker et al., 1972). The curve differs little from that obtained at the $g_\perp$ setting and is typical of the results obtained with hydrated complexes of other paramagnetic ions (Mims and Davis, 1976). Its general features have been explained by assuming an approximately spherical distribution of hydrogen nuclei surrounding the paramagnetic ion. (This approximation, though perhaps a poor one in the case of a single crystal sample, is acceptable for a glass, in which the paramagnetic complexes are oriented at random.) The ≃90-ns period observable at the beginning of the trace corresponds to the proton precession period in the Zeeman field. Since the proton frequencies are shifted in varying amounts owing to the proximity of the Cu(II) magnetic moment, the corresponding signals tend to interfere and the ≃90-ns period decays rapidly, having almost disappeared by the end of the trace. The shorter period ≃45-ns that dominates the pattern towards the end corresponds to the sum of the two ENDOR frequencies associated with the upper and lower electron spin levels (see eq 45 in Mims, 1972a) and is approximately twice the proton frequency. Since the dipolar coupling contributes opposite shifts in the two ENDOR intervals this sum frequency is more nearly monochromatic and persists for a longer period in the time waveform than the proton frequency itself.

The curve in Figure 5 shows the echo envelope for the Cu(II)–glycylglycine complex at pH 8.5, the immediate ligands in this case being oxygen (2 ligands) and imino and amino nitrogen (1 ligand each) (Freeman, 1966; Crawford and Dalton, 1969). The ^{14}N nuclei belonging to the imino and amino ligands make no contribution to the modulation envelope here, indicating that in this case the I·A·S term exceeds

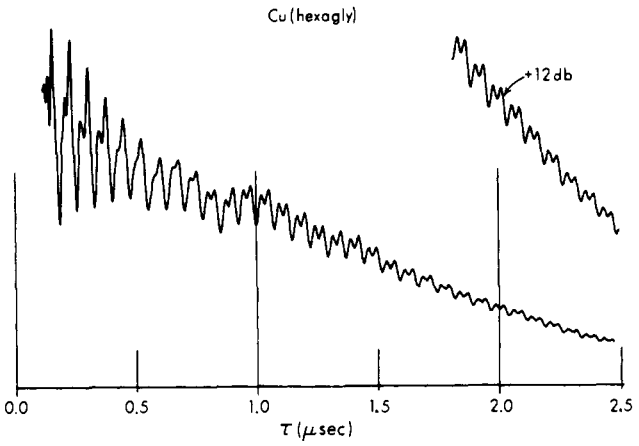

FIGURE 7: Envelope modulation function for Cu(II)-hexaglycine prepared at pH 6.0. Conditions were similar to those in Figure 4. The major features in the spectrum show the effect of proton coupling, similar to that seen for hydrated Cu(II) (Figure 4) or for Cu(II)-glycylglycine (Figure 5). The weak feature observed near 1 μs is ascribed to interaction with nitrogen atoms not directly ligated to copper.

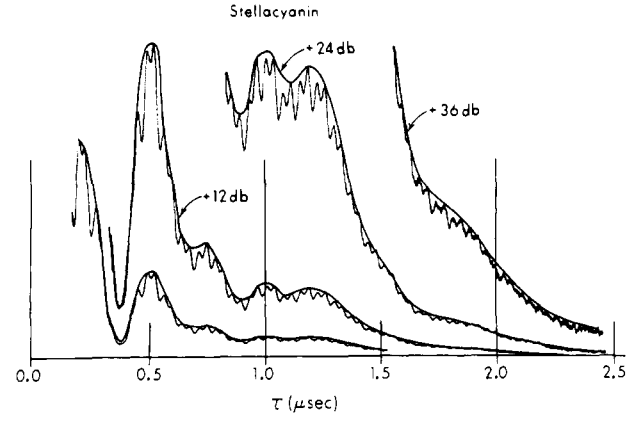

FIGURE 8: Envelope modulation function for stellacyanin. Conditions were similar to those in Figure 6. The low-frequency period is assigned to an imidazole ligand as in Figure 6.

the Zeeman term ($\simeq$1 MHz) and the ^{14}N quadrupole terms ($\simeq$1-2 MHz; Edmonds and Summers, 1973; Hunt, 1974) by a comfortable margin. This is not surprising, since, in the analogous case of the Cu(II)-*o*-phenanthroline dichloride complex $A_{\parallel,Cl}$ = 36 MHz and $A_{\perp,Cl}$ = 26 MHz (Kokoszka et al., 1967).

The echo envelope for the Cu(II)-bovine serum albumin complex in Figure 6 shows a new low-frequency component in addition to the high-frequency proton components observed in Figures 4 and 5. Studies have shown that in this case, the Cu(II) ion is coordinated by one amino nitrogen, two peptide nitrogens, and one nitrogen from an imidazole group (Peters and Blumenstock, 1967). The new modulation period is presumably due to the imidazole ligand, since, as we have seen in the preceding case (Figure 5), nuclear coupling with the ^{14}N in an amino or imino ligand is not observable in echo envelope experiments. It seems probable, moreover, that the nitrogen responsible for the modulation pattern is the N-1 nitrogen of the imidazole group rather than the N-3 nitrogen that coordinates the Cu(II) ion directly. Coupling between the Cu(II) ion and the remote nitrogen nucleus is more likely to be of the correct order of magnitude to contribute to echo envelope modulation (i.e., to be comparable with the quadrupole and Zeeman couplings).

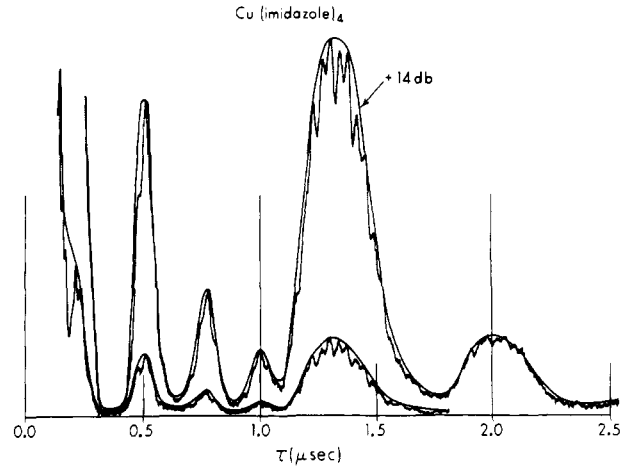

FIGURE 9: Envelope modulation function for the compound Cu(II)-(imid)$_4$. Conditions were similar to those in Figure 6. This curve is reproduced for comparison with the curve in Figure 10.

The low-frequency modulation period ascribed to imidazole in Cu(II)-bovine serum albumin cannot arise from close lying peptidic or amino nitrogen. Recordings of the spin-echo envelope for Cu(II)-hexaglycine prepared at pH 7.0 or 9.5 show that the modulation pattern is essentially the same as that which is observed for hydrated Cu(II) (Figure 4) or for Cu(II)-glycylglycine (Figure 5). However, for the Cu(II)-hexaglycine sample prepared at pH 6.0 (Figure 7) the pattern contains a shallow modulation feature near 1.0 μs that is attributed to interaction with nitrogen not directly bonded with the copper. As can be seen, the depth of nitrogen modulation here is considerably less than for Cu(II)-serum albumin (Figure 6).

The echo envelope for stellacyanin is shown in Figure 8. As can be seen, there is a low frequency modulation pattern with features that show a close correspondence to those obtained for the Cu(II)-bovine serum albumin complex, and it is primarily on these grounds that we assign an imidazole ligand to the copper of stellacyanin. In addition, the high-frequency component ascribed to protons is less pronounced for stellacyanin than it is for Cu(II)-bovine serum albumin suggesting that there are less protons near the copper in stellacyanin than in the copper albumin complex.

Although our findings suggest copper coordination to an imidazole ligand in stellacyanin, it would be useful to be able to exclude the possibility of coordination by a guanidine residue from arginine, since this ligand would, like imidazole, contain nitrogen atoms twice removed from Cu(II) in addition to a directly coordinating nitrogen atom. Unfortunately, in this case we were not able to obtain a suitable model with a single guanidyl ligand to copper, but some evidence excluding the possibility of a guanidyl ligand in stellacyanin can be obtained by comparing the echo envelopes for the complexes Cu(II)(imid)$_4$ and Cu(II)(guan)$_4$ in Figures 9 and 10, respectively. The curve for Cu(II) (imid)$_4$ is different in appearance from the curve for Cu(II)-bovine serum albumin (Figure 6) where the Cu(II) is coordinated by only one imidazole ligand, but, from the maxima associated with the low-frequency component (at $\simeq$0.5, 0.7, 1.1, 1.3, and 2.0 μs), it can be seen that it is generated by similar superhyperfine couplings. The Cu(II)-(guan)$_4$ curve (Figure 10) differs markedly from the Cu(II)-(imid)$_4$ curve (Figure 9), indicating that there is little likelihood of mistaking the pattern due to guanidyl ligands for the pattern due to imidazole ligands.

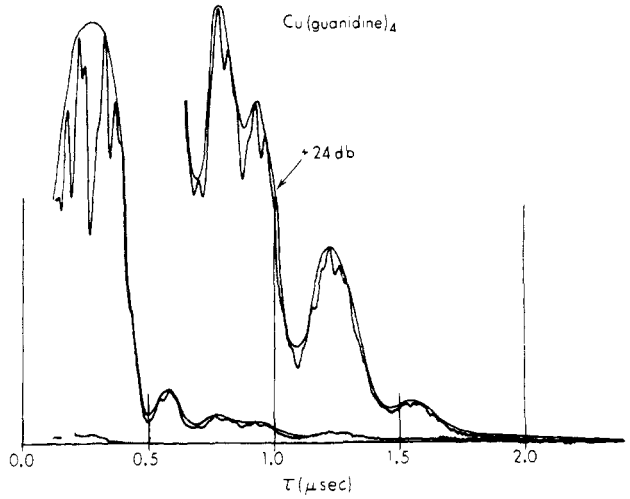

FIGURE 10: Envelope modulation function for the compound Cu(II) $(guan)_4$. Conditions were similar to those in Figure 6. Comparison with Figure 9 shows that coupling between Cu(II) and the remote ^{14}N nuclei in the guanidine ligands results in a pattern that is quite different from that resulting from coupling between Cu(II) and the N-1 nitrogens in imidazole ligands.

These results leave open the question as to the number of imidazole ligands coordinating Cu(II) in stellacyanin. In general, it is true that the more the equivalent groups, the deeper the modulation pattern,[2] but it is necessary to have some more specific information as to the relative orientations of the ligands before one is able to analyze results quantitatively in this way. From a rough comparison of Figures 9 and 10 we should infer that one imidazole ligand is the more likely assignment, though the possibility of there being two cannot be ruled out.

In summary, we have shown how the nuclear modulation effect in pulsed EPR spectroscopy gives new types of information about paramagnetic centers in biomolecules. This technique provides a useful means for identifying nuclei in the neighborhood of a paramagnetic center and can also in certain cases be used to identify the ligands of metal ions in proteins.

References

Andreasson, L-E, and Vänngård, T. (1970), *Biochim. Biophys. Acta 200,* 247–257.

Blumberg, W. E., Eisinger, J., Aisen, P., Morell, A. G., and Scheinberg, I. H. (1963), *J. Biol. Chem. 238,* 1675–1682.

Blumberg, W. E., Levine, W. G., Margolis, S., and Piesach, J. (1964), *Biochem. Biophys. Res. Commun. 15,* 277–283.

Blumberg, W. E., Mims, W. B., and Zuckerman, D. (1973), *Rev. Sci. Instrum. 44,* 546–555.

Blumberg, W. E., and Peisach, J. (1966), *Biochim. Biophys. Acta 126,* 269–273.

Brill, A. S., Bryce, G. F., and Maria, H. (1968), *Biochim. Biophys. Acta 154,* 342–351.

Crawford, T. H., and Dalton, J. O. (969), *Arch. Biochem. Biophys. 131,* 123–128.

Edmonds, D. T., and Summers, C. P. (1973), *J. Magn. Reson. 12,* 134–142.

Finazzi-Agró, A., Rotilio, G., Avigliano, L., Guerrieri, P., Boffi, V., and Mondovì, B. (1970), *Biochemistry 9,* 2009–2014.

Freeman, H. C. (1966), in The Biochemistry of Copper, Peisach, J., Aisen, P., and Blumberg, W. E. Ed., New York, N.Y., Academic Press, pp 77–113.

Gould, D. C., and Mason, H. S. (1967), *Biochemistry 6,* 801–809.

Grischkowsky, D., and Hartmann, S. R., (1970), *Phys. Rev. B 2,* 60–74.

Hunt, M. J. (1974), *J. Magn. Reson. 15,* 113–121.

Katoh, S., Shiratori, T., and Takamiya, A. (1962), *J. Biochem. 51,* 32–40.

Kevan, L., Bowman, M. K., Narayana, P. A., Boechman, R. K., Yudanov, V. F., and Tsvetkov, Yu. D. (1975), *J. Chem. Phys. 63,* 409–416.

Kokoszka, C. W., Reimann, C. W., and Allen, H. C. (1967), *J. Phys. Chem. 71,* 121–126.

Liao, P. F., and Hartmann, S. R. (1972), *Solid State Commun. 10,* 1089–1091.

Malkin, R., Malmström, B. G., and Vänngård, T. (1968a), *Eur. J. Biochem. 10,* 324–329.

Malkin, R., Malmström, B. G., and Vänngård, T. (1968b), *FEBS Lett. 1,* 50–54.

Malmström, B. G., Reinhammer, B., and Vänngård, T. (1968), *Biochim. Biophys. Acta 156,* 67–76.

Malmström, B. G., Reinhammar, B., and Vänngård, T. (1970), *Biochim. Biophys. Acta 205,* 48–57.

Malmström, B. G., and Vänngård, T. (1960), *J. Mol. Biol. 2,* 118–124.

McMillin, D. R., Holwerda, R. A., and Gray, H. B. (1974), *Proc. Natl. Acad. Sci. U.S.A. 71,* 1339–1341.

Mims, W. B. (1972a), *Phys. Rev. B 5,* 2409–2419.

Mims, W. B. (1972b), *Phys. Rev. B 6,* 3543–3545.

Mims, W. B. (1972c), in Electron Paramagnetic Resonance, Geschwind S., Ed., New York, N.Y., Plenum Press, pp 263–351.

Mims, W. B. (1974), *Rev. Sci. Instrum. 45,* 1583–1591.

Mims, W. B., and Davis, J. L. (1976), *J. Chem. Phys. 64,* 4836–4846.

Nakamura, T., Makino, N., and Ogura, Y. (1968), *J. Biochem. (Tokyo) 64,* 189–195.

Nakamura, T., and Ogura, Y. (1966), *J. Biochem. 59,* 449–455.

Narayana, P. A., Bowman, M. K., Kevan, L., Yudanov, V. F., and Tsvetkov, Yu. D. (1975), *J. Chem. Phys. 63,* 3365–3371.

Newman, F. C., and Rowan, L. G., (1972), *Phys. Rev. B 5,* 4231–4236.

Omura, T. (1961), *J. Biochem. (Tokyo) 50,* 394–399.

Peisach, J., and Blumberg, W. E. (1975), *Arch. Biochem. Biophys. 162,* 502–512.

Peisach, J., and Levine, W. G. (1965), *J. Biol. Chem. 240,* 2284–2289.

Peisach, J., Levine, W. G., and Blumberg, W. E. (1967), *J. Biol. Chem. 242,* 2847–2858.

Peters, T., and Blumenstock, F. A. (1967), *J. Biol. Chem. 242,* 1574–1578.

Poillon, W. N., and Dawson, C. R. (1963), *Biochim. Biophys. Acta 77,* 37–46.

Reinhammar, B. (1970), *Biochim. Biophys. Acta 205,* 35–47.

Rist, G. H., Hyde, J. S., and Vänngård, T. (1970), *Proc. Natl. Acad. Sci. U.S.A. 67,* 79–86.

[2] This follows from the product theorem that governs the form of the echo envelope in cases where there is coupling to more than one nucleus. See, e.g., eq 42 in Mims (1972a).

Rowan, L. G., Hahn, E. L., and Mims, W. B. (1965), *Phys. Rev. A 137,* 61–71.
Stigbrand, T., Malmström, B. G., and Vänngård, T. (1971), *FEBS Lett. 12,* 260–262.
Sutherland, I. W., and Wilkinson, J. F. (1963), *J. Gen. Microbiol. 30,* 105–112.
Suzuki, H., and Iwasaki, H. (1962), *J. Biochem. (Tokyo) 52,* 193–199.
Walker, F. A., Sigel, H., and McCormick, D. B. (1972), *Inorg. Chem. 11,* 2756–2763.
Yudanov, V. F., Raitsimring, A. M., Tsvetkov, Yu. D. (1968), *Theor. Exp. Chem. 4,* 335–341.
Zhidomirov, G. M., and Salikhov, K. M. (1968) *Theor. Exp. Chem. 4,* 332–334.

Comparison of the Phosphorus Magnetic Resonance and Circular Dichroism Properties of Calf Thymus DNA and Chromatin†

Sue Hanlon,* Thomas Glonek, and Aurelia Chan

ABSTRACT: Dual measurements of the ^{31}P magnetic resonance spectra and the circular dichroism spectra have been made on calf thymus DNA and purified chromatin. The ^{31}P magnetic resonance signals for all samples fell at 1.2 ± 0.1 ppm relative to 85% orthophosphoric acid. The full width at half-height of the signal of samples in which the molecular weight of the native DNA component was in the 2–9 × 10^6 range was ca. 50 Hz. This bandwidth was reduced dramatically to ca. 20 Hz by reducing the molecular weight to 140 000 (by sonication) or by heat denaturation of the high-molecular-weight DNA. The position of the signal and the bandwidth of the chromatin samples did not differ significantly from that of the DNA samples of comparable molecular weight and state of nativity. The intensities of the chromatin signals, however, were all less than those of signals of DNA in companion runs conducted under comparable experimental conditions. The reduction of the intensity of the magnetic resonance signal paralleled the lowering of the intensity of the positive band above 260 nm in the circular dichroism spectrum of the given sample of chromatin relative to the spectrum of protein-free DNA. In fact, the percent reduction of the magnetic resonance signal of chromatin relative to protein-free DNA was, within experimental error, equal to the percentage of nucleotide residues in the Watson–Crick B secondary structure. Since the latter fraction of residues can be correlated with those in the interbead regions of the superstructure of chromatin, we have concluded that the signal of the nucleotide residues in the beads, or υ bodies, has been broadened to the point of extinction by a packing arrangement which maximizes phosphate–protein interactions and structural rigidity.

In preceding papers from this laboratory we have proposed a model for purified calf thymus chromatin in which the DNA constituent is in two discrete secondary structures. As ascertained by circular dichroism (CD)[1] spectral analysis, anywhere from 30 to 50% of the nucleotide residues are in a form resembling the Watson–Crick B conformation, whereas the remainder are in a C conformation, which is a helical variant of the B form. The distribution of residues between the two conformations can be varied by several methods. Exhaustive dialysis against EDTA,[1] high concentrations of denaturants such as urea, proteolytic digestion, and removal of histone proteins with dissociative reagents such as sodium deoxycholate or NaCl will result in substantial increases in the B character at the expense of the C (Hanlon et al., 1974a), whereas nuclease digestion (with subsequent removal of the low-molecular-weight products of digestion) results in a macromolecular product which displays a CD spectrum almost identical to that exhibited by the C form of DNA (Hanlon et al., 1972; Johnson et al., 1972; Rill and Van Holde, 1973; Hanlon et al., 1975). The arguments in favor of discrete conformations in intact chromatin have included the results of this latter experiment, as well as the almost exact correlation between the %B character and the fraction of bases melting out in the lower transition regions of the complex melting profile which is exhibited by purified chromatin (Hanlon et al., 1972, 1974b; Johnson et al., 1972).

Electron microscopic observations on chromatin from interphase nuclei have revealed a structure resembling "beads on a string" (Olins and Olins, 1974). The beads, referred to as υ bodies by Olins and Olins (1974), can be produced by nuclease treatment (Van Holde et al., 1974; Finch et al., 1975) or extensive sonication (Senior et al., 1975). Since the products of digestion by nucleases have a CD spectrum which is almost identical with C spectrum DNA above 250 nm (Johnson et al., 1972; Rill and Van Holde, 1973), it is reasonable to conclude that the DNA in the "beads" or υ bodies is in the C conformation, whereas the DNA in the interbead or string regions of intact chromatin is in the B conformation (Hanlon, S., Berman, S., and Chan, A., in preparation).

A further aspect of our model includes the limited accessibility of the portions of chromatin in which DNA is in the C form. These regions are resistant to nuclease digestion and seem to be very well stabilized to heat denaturation as they melt in the high T_m transitions of the thermal melting profile of chromatin (Johnson et al., 1972; Rill and Van Holde, 1973).

† From the Department of Biological Chemistry, College of Medicine, and the Research Resources Center of the University of Illinois at the Medical Center, Chicago, Illinois (60612). *Received February 19, 1976.* This work was supported by Grant BMS 75-16488 from the National Science Foundation, and Grant PHS-GRSG 615 from the National Institutes of Health.

[1] Abbreviations used are: EDTA, the sodium salt of (ethylenedinitrilo)tetraacetic acid; CD, circular dichroism; Tris, 2-amino-2-hydroxymethyl-1,3-propanediol; TNH, purified chromatin.